SEX DIFFERENCES IN THE HUMAN CONNECTOME: 4-TESLA HIGH ANGULAR RESOLUTION DIFFUSION IMAGING (HARDI) TRACTOGRAPHY IN 234 YOUNG ADULT TWINS

Neda Jahanshad[1], Iman Aganj[2], Christophe Lenglet[3,2], Anand Joshi[1], Yan Jin[1], Marina Barysheva[1], Katie L. McMahon[4], Greig I. de Zubicaray[5], Nicholas G. Martin[6], Margaret J. Wright[5,6], Arthur W. Toga[1], Guillermo Sapiro[2], Paul M. Thompson[1]

[1]Laboratory of Neuro Imaging, Department of Neurology, UCLA School of Medicine, Los Angeles, CA
[2]Department of Electrical and Computer Engineering, University of Minnesota, Minneapolis, MN
[3]Center for Magnetic Resonance Research, University of Minnesota Medical School, Minneapolis, MN
[4]University of Queensland, Centre for Advanced Imaging, Brisbane, Australia
[5]University of Queensland, School of Psychology, Brisbane, Australia
[6]Queensland Institute of Medical Research, Brisbane, Australia

ABSTRACT

Cortical connectivity is associated with cognitive and behavioral traits that are thought to vary between sexes. Using high-angular resolution diffusion imaging at 4 Tesla, we scanned 234 young adult twins and siblings (mean age: 23.4 ± 2.0 SD years) with 94 diffusion-encoding directions. We applied a novel Hough transform method to extract fiber tracts throughout the entire brain, based on fields of constant solid angle orientation distribution functions (ODFs). Cortical surfaces were generated from each subject's 3D T1-weighted structural MRI scan, and tracts were aligned to the anatomy. Network analysis revealed the proportions of fibers interconnecting 5 key subregions of the frontal cortex, including connections between hemispheres. We found significant sex differences (147 women/87 men) in the proportions of fibers connecting contralateral superior frontal cortices. Interhemispheric connectivity was greater in women, in line with long-standing theories of hemispheric specialization. These findings may be relevant for ongoing studies of the human connectome.

Index Terms— tractography, high angular resolution diffusion imaging (HARDI), network analysis, inter-hemispheric connectivity, human connectome

1. INTRODUCTION

The organization of white matter fiber pathways connecting the two cerebral hemispheres is of great interest when studying normal development as well as neurological and psychiatric disorders such as Alzheimer's disease [1] and schizophrenia [2].

Differences in cortical connectivity between men and women may also contribute to reported sex differences in traits such as linguistic processing [3] and general cognition [4]. Both of these measures have been associated with connectivity metrics in women but not in men [3,4]. Tractography studies based on diffusion tensor imaging have also been applied to subdivide the inter-hemispheric fibers of the corpus callosum into functionally organized sectors or tracts, based on the cortical regions that the fibers interconnect [5]. Chao et al. [6] used high angular resolution diffusion imaging (HARDI) to derive tracts, and studied interhemispheric connections passing through the corpus callosum to parcellate its structure.

In a small sample of 5 subjects, Hagmann et al. [7] showed network connectivity maps for fibers connecting cortical regions within and across hemispheres using high-resolution tractography based on diffusion spectrum imaging (DSI). In their study, the majority of connections were found to be between regions within rather than across hemispheres.

Here we used a novel HARDI tractography algorithm based on the Hough transform [8] to extract tracts throughout the entire brain. In a large cohort of 234 young healthy subjects scanned with HARDI, we seeded voxels with a probability proportional to the fractional anisotropy (FA) measured at each voxel, derived (for simplicity) from the single-tensor model of diffusion. We then examined the interhemispheric connection matrix, and its statistical variation in 36 monozygotic (MZ) and 28 same-sex dizygotic (DZ) twin pairs. We set out to discover genetic influences and any sex differences in the population of connectivity matrices.

The human frontal lobes mediate or influence a broad variety of behaviors. These include executive function, working memory, problem solving, judgment, motor planning, speech production, impulse control, and some aspects of social behavior. The frontal lobe is also heavily interconnected. Many voxels contain white matter fiber mixings and crossings. These fiber crossings may not be correctly captured by tractography methods based on the single-tensor diffusion model, so higher order modeling of the diffusion propagator with HARDI becomes advantageous. Using the entire set of 234 subjects, we examined sex differences in the extent of interhemispheric fiber connectivity between cortical regions in the frontal lobes. As aberrant connectivity is implicated in various brain disorders, sex differences in connectivity may also be important to recognize, in ongoing projects to map the human connectome.

2. METHODS

2.1. Subject Demographics and Image Acquisition

As part of a large-scale imaging genetics initiative focusing on twins [9], we scanned 234 young adults (147 women/87 men; mean age: 23.4 ± 2.0 SD years) with 4T HARDI and standard T1-weighted structural MRI. To examine genetic and environmental influences on brain connectivity, the participants were all twin subjects and their siblings from 131 families. All MR images were collected using a 4 Tesla Bruker Medspec MRI scanner (Bruker Medical, Ettingen, Germany), with a transverse electromagnetic (TEM) headcoil, at the Center for Magnetic Resonance (University of Queensland, Australia). T1-weighted images were acquired with

an inversion recovery rapid gradient echo sequence (TI/TR/TE = 700/1500/3.35 ms; flip angle=8°; slice thickness = 0.9 mm, with a 256^3 acquisition matrix). Diffusion-weighted images were acquired using single-shot echo planar imaging with a twice-refocused spin echo sequence to reduce eddy-current induced distortions. Imaging parameters were: TR/TE 6090/91.7 ms, 23 cm FOV, with a 128×128 acquisition matrix. Each 3D volume consisted of 55 2-mm thick axial slices with no gap, and a 1.79×1.79 mm^2 in-plane resolution. We acquired 105 images per subject: 11 with no diffusion sensitization (i.e., T2-weighted b_0 images) and 94 diffusion-weighted (DW) images (b = 1159 s/mm^2) with gradient directions evenly distributed on the hemisphere, as is required for unbiased directional sampling of the diffusion propagator. Scan time was 14.2 minutes.

2.2. DWI preprocessing, cortical surface extractions and registrations

Non-brain regions were automatically removed from each T1-weighted MRI scan, and from a T2-weighted image from the DWI set using the FSL tool "BET" (http://fsl.fmrib.ox.ac.uk/fsl/). A trained neuroanatomical expert manually edited the T1-weighted scans to further refine the brain extraction. All T1-weighted images were linearly aligned using FSL (with 9 DOF) to a common space [10] with 1mm isotropic voxels and a 220×220×220 voxel matrix. Raw diffusion-weighted images were corrected for eddy current distortions using the FSL tool, "eddy_correct" (http://fsl.fmrib.ox.ac.uk/fsl/). For each subject, the 11 eddy-corrected images with no diffusion sensitization were averaged, linearly aligned and resampled to a downsampled version of their corresponding T1 image (110×110×110, 2×2×2mm). Averaged b_0 maps were elastically registered to the structural scan using a mutual information cost function [11] to compensate for EPI-induced susceptibility artifacts.

Table 1: List of the cortical labels extracted from FreeSurfer [11]; label 1 was reserved for non-cortical surfaces.

1	Banks of the superior temporal sulcus	19	*Pars orbitalis*
2	Caudal anterior cingulate	20	*Pars triangularis*
3	Caudal middle frontal	21	Peri-calcarine
4	Corpus callosum	22	Postcentral
5	Cuneus	23	Posterior cingulate
6	Entorhinal	24	Pre-central
7	Fusiform	25	Precuneus
8	Inferior parietal	26	Rostral anterior cingulate
9	Inferior temporal	27	Rostral middle frontal
10	Isthmus of the cingulate	28	Superior frontal
11	Lateral occipital	29	Superior parietal
12	Lateral orbitofrontal	30	Superior temporal
13	Lingual	31	Supra-marginal
14	Medial orbitofrontal	32	Frontal pole
15	Middle temporal	33	Temporal pole
16	Parahippocampal	34	Transverse temporal
17	Paracentral	35	Insula
18	*Pars opercularis*		

35 cortical labels per hemisphere (**Table 1**) were automatically extracted from all aligned T1-weighted structural MRI scans using FreeSurfer (http://surfer.nmr.mgh.harvard.edu/) [12]. As a linear registration is performed within the software, the resulting T1-weighted images and cortical models were aligned to the original T1 input image space and down-sampled using nearest neighbor interpolation (to avoid intermixing of labels) to the space of the DWIs. To ensure tracts would intersect cortical labeled boundaries, labels were dilated with an isotropic box kernel of 5 voxels.

2.3. HARDI tractography

The transformation matrix from the linear alignment of the mean b_0 image to the T1-weighted volume was applied to each of the 94 gradient directions to properly re-orient the orientation distribution functions (ODFs). At each HARDI voxel, ODFs were computed using the normalized and dimensionless ODF estimator, derived for QBI in [13]. Contrary to prior methods, this approach considers the Jacobian factor r^2 to compute the constant solid angle (CSA) ODF:

$$\underset{\text{in CSA-QBI}}{ODF}(\hat{u}) \approx \frac{1}{4\pi} + \frac{1}{16\pi^2}\,\mathrm{FRT}\left\{\nabla_b^2 \ln\left(-\ln\frac{S(\hat{u})}{S_0}\right)\right\}$$

Here $S(\hat{u})$ is the diffusion signal, and S_0 is the baseline image. FRT is the Funk-Radon transform and ∇_b^2 is the Laplace-Beltrami operator. We used this ODF reconstruction scheme as it is mathematically more accurate and also outperforms the original QBI definition [14], e.g., it improves the resolution of multiple fiber orientations [13]. With this set of ODFs, we performed HARDI tractography on the linearly aligned sets of DWI volumes.

Tractography was performed by probabilistically seeding voxels with a prior probability based on the fractional anisotropy (FA) value derived from the single-tensor model [15]. All curves passing through a seed point receive a score estimating the probability of the existence of the fiber, computed from the ODFs. We used a voting process provided by the Hough transform to determine the best fitting curves through each point. Further details of the method may be found in [8].

Elastic deformations obtained from the EPI distortion correction, mapping the average b_0 image to the T1-weighted image, were then applied to the tract's 3D coordinates. As this was a study of inter-hemispheric connectivity, tracts with fewer than 15 points were filtered out. Each subject's dataset contained 2000-4000 useable fibers (3D curves).

2.4. *N*x*N* frontal lobe connectivity analysis

For each subject, a full 70×70 connectivity matrix was created. Each element described the estimated proportion of the total number of fibers, in that subject, connecting each of the labels in one hemisphere to those in the other hemisphere. If more than 5% of subjects had no fibers connecting the regions, then the connection was considered invalid and was not included in the analysis.

To further focus our analyses, 5 cortical regions of interest (ROIs) were selected from the frontal lobes in each hemisphere. These regions included: (1) the caudal middle frontal, (2) lateral orbito- frontal, (3) rostral anterior cingulate, (4) superior frontal, and (5) insular, cortical surface labels. **Figure 1** shows these 5 ROIs in one representative subject. A 10×10 normalized connectivity matrix was created for each subject. This encodes the proportion of the total number of fibers, in that subject, connecting each of the 5 ROIs in one hemisphere to each other as well as across hemispheres.

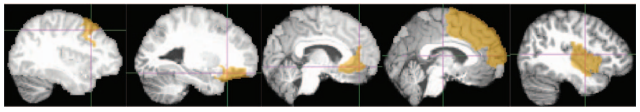

Figure 1: Hemispheric frontal lobe regions of interest included, from left to right: (1) the caudal middle frontal, (2) lateral orbito-frontal, (3) rostral anterior cingulate, (4) superior frontal, and (5) insular, cortical surface labels.

Similarities may arise in the tractography maps as individuals in the same family are related; therefore, we used a random-effects regression analysis to group the subjects by family. A random intercept was included for each family. The analysis was performed covarying for the effect of age. Sex (coded as 1 - male and 2 - female) was regressed on each valid matrix connection.

To obtain an accurate estimate of sex differences in brain connectivity, a nonparametric test was performed using 5,000 random permutations of the sex of each individual and repeating the regression. Constraints were applied to ensure that all monozygotic twin pairs remained of the same sex, in the randomly permuted sex assignments. As such, the permutation test was valid and sensitive to genetic differences other than sex differences. The analysis was implemented using the 'nlme' library, in the R statistical package (version 2.9.2; http://www.r-project.org/) [16].

2.5. Falconer's heritability analysis

Falconer's heritability analysis was performed using a subset of the population— 36 (25F) monozygotic twin pairs, and 28 (19F) same-sex dizygotic twin pairs. The heritability of each valid connection was then determined according to Falconer's heritability estimate [17]: $h^2=2(rMZ - rDZ)$. Here, *rMZ* and *rDZ* denote the intraclass correlation (ICC) coefficients for monozygotic and dizygotic twins; heritability denotes the proportion of the observed variation that is attributable to genetic differences among individuals. To assess the significance of the measures of familial resemblance, the false discovery rate (FDR) was controlled at q=0.05 for p-values corresponding to the observed MZ twin correlations.

3. RESULTS

Figure 2 shows the full map of the dilated cortical surface labels of one subject's left hemisphere overlaid on top of their T1-weighted image. The EPI-corrected map of the fiber density is also directly overlaid to show that the DWI-derived fibers are accurately registered to the structural scan.

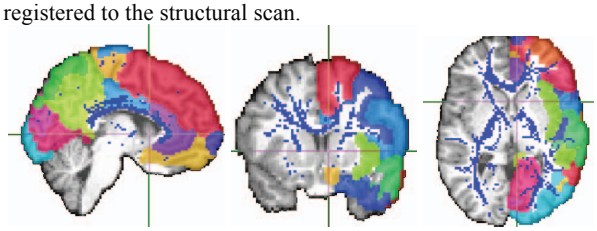

Figure 2: Cortical surface labels from a representative subject's left hemisphere are overlaid on sections from the same subject's 3D T1-weighted image. The EPI-corrected map of the fiber density is also overlaid. This shows that the DWI-derived fibers are accurately registered to the structural scan.

The proportion of fibers that form the full hemispheric cortical connectivity matrix, averaged across all subjects in the study, is plotted in **Figure 3.** In agreement with [7], most connections were found to be within the same hemisphere. 4 valid interhemispheric connections were observed: (1) between the right and left precuneus (2) the right precuneus and the left isthmus of the cingulate, (3) the left precuneus and the right isthmus of the cingulate, and (4) the left and right posterior cingulate. On average, about 15% of the inter-hemispheric fibers connect the left and right precuneus regions of the cortex (region 25). In these estimates, we note a minor bias that fiber selection was weighted toward seed voxels with high FA, but was not biased towards any one region, unless it had higher FA in aggregate.

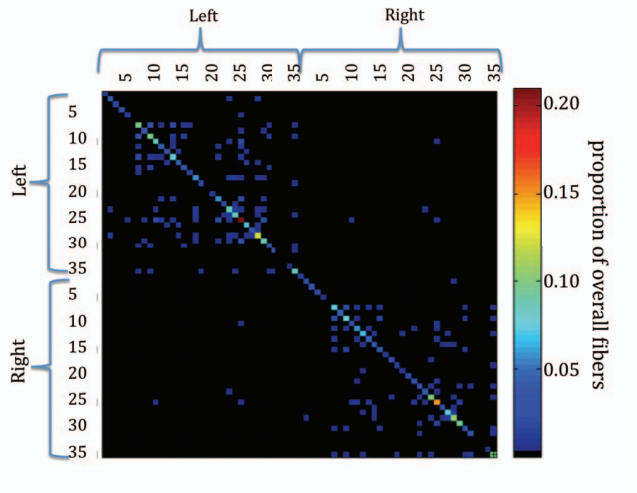

Figure 3: Averaged across all 234 subjects, here we show the proportion of fibers that form the full inter-hemispheric cortical connectivity matrix. In agreement with [7], most connections are within the same hemisphere. On average, about 15% of the fibers traced here interconnect both the left (label number 25) and right (label number 60) precuneus regions of the cortex, and 10% the insula (labels 35 and 70).

After Bonferroni correction for the statistical tests conducted on consistently identified connections within the frontal lobe, significant ($p < 0.0033$) sex differences were found in the inter-hemispheric connectivity of the superior frontal cortices, with women showing higher connectivity than men. Men had a significantly higher proportion of connections within the right lateral orbito-frontal cortex and more fibers interconnecting this region with the ipsilateral insula. Permutation corrected p-values are shown in **Figure 4.**

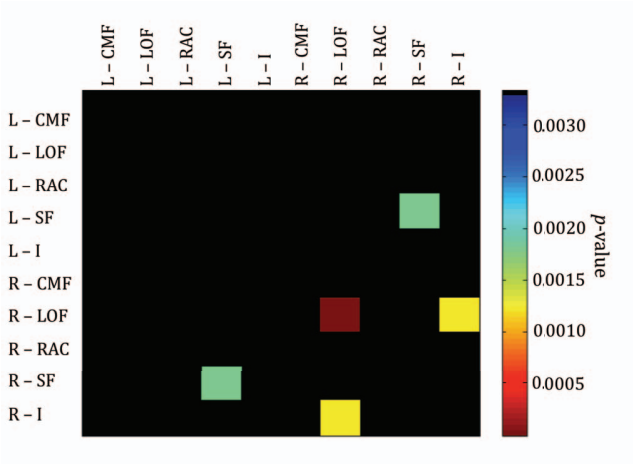

Figure 4: Significant ($p < 0.0033$) sex differences were found in the inter-hemispheric connectivity of the superior frontal cortices, with women showing higher connectivity. Men had a significantly higher proportion of connections within the right lateral orbito-frontal cortex and more fibers interconnecting this region with the ipsilateral insula.

A cumulative distribution plot of the significance of the MZ and DZ correlations is shown in **Figure 5** highlighting the significance in the correlations between the monozygotic pairs as opposed to the dizygotic twins within the valid connections (where at least 95% of all subjects had tracts), providing strong evidence for heritability. Falconer's heritability estimates are displayed for these consistently found connections, in **Figure 6**. The most heritable fiber counts were those in the left precuneus, fibers connecting the cortical regions of the left peri-calcarine and fusiform gyri, and those of the left cuneus and precuneus, also showed moderate heritability (10-12%). When the analysis was limited to only female twin pairs, very high heritability (73%) was found for the fibers interconnecting the left insula with the left superior temporal regions. No other connections were found to be heritable in the female subpopulation. Analysis restricted to men was not performed due to the limited number of male-only twin pairs in each group (11 MZ pairs, 9 DZ pairs).

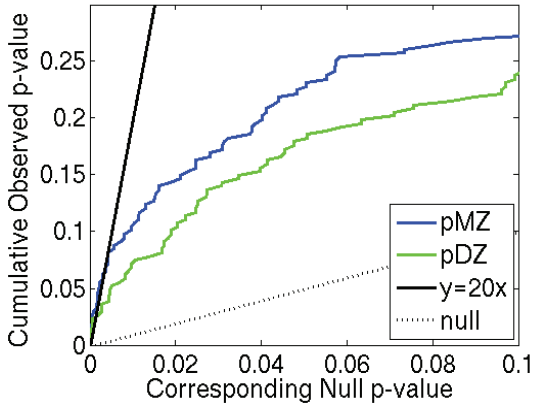

Figure 5: Cumulative distribution plots of the intraclass correlation probabilities within each group of twins. As expected for genetically influenced traits, correlation effects are greater for monozygotic twins than dizygotic twins. This suggests the presence of genetic influences on cortical connectivity that can be further analyzed by modeling heritability.

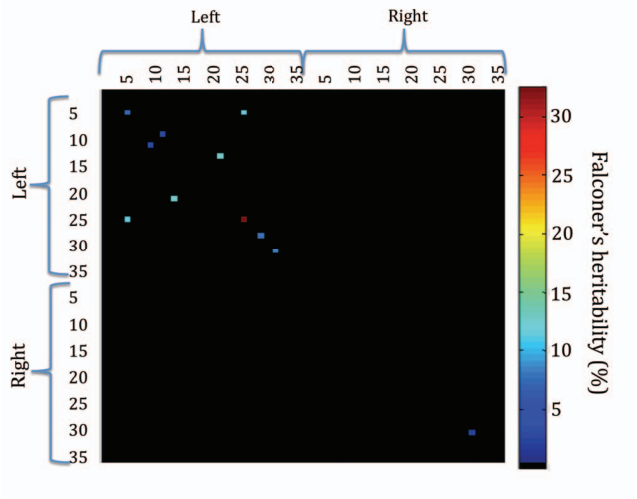

Figure 6: The heritability matrix is shown. Color values in the cells show the heritability coefficient for each valid (consistently found) connection. The heritability matrix shows regions of significant heritability in the left hemisphere, with highest levels (~32%) for the fiber counts of the left precuneus. Fibers connecting cortical regions of the left peri-calcarine and fusiform gyri, and those of the left cuneus and precuneus, also showed moderate heritability (10-12%).

4. DISCUSSION

In this study, we used 94-direction high-angular resolution images (HARDI) in 234 individuals at 4 Tesla, to trace fiber tracts throughout the entire brain. We used a novel orientation distribution function (ODF) based tractography method to account for crossing fibers, allowing valid pursuit of the diffusion propagator where fibers mix or cross. Cortical labels were extracted automatically from co-registered surface models, and the proportion of interhemispheric connections was further studied, using statistical analysis of the connectivity matrices.

In our heritability analysis for cortical fiber connectivity, we observed moderate (33%) levels of heritability for the fiber proportions innervating the left precuneus in the full group. However, when the analysis was limited to only female twin pairs, high heritability (73%) was found in the fibers interconnecting the left insula with the left superior temporal regions. When larger samples are available, we will be able to assess interactions between sex and heritability, and model environmental sources of variance using structural equation models.

The frontal lobe has a high proportion of voxels containing white matter fibers that mix or cross. This leads to fiber incoherence and partial volume effects in the large voxels typical of diffusion-weighted images. Tracts in these regions are challenging to trace accurately using the standard single-tensor model. The principal direction of the tensor can be misleading when fibers mix or cross in the same voxel, so here we used a full ODF model of the HARDI signal, to better capture fiber trajectories. The use of higher magnetic fields with smaller voxel sizes might lead to further improvements.

The human frontal lobe is critical for mediating executive function, self-control, and speech. As there is also some evidence for sex-dependent functioning, we examined sex differences in the intra- and inter-hemispheric circuitry of 5 key frontal lobe cortical regions using ODF-based whole-brain HARDI tractography. In line with some theories of hemispheric specialization and sex differences [18-20], we were able to find significant sex differences in the white matter fiber counts. Women had a greater proportion of connections between left and right superior frontal cortices. They also had fewer fibers overall within the right lateral orbito-frontal region. We previously found sex differences in the geometric complexity of these cortical regions, using fractal dimension analysis, in a separate cohort [21].

In this study, we did not normalize the fiber counts to account for differences in the sizes of the cortical regions within the brain and across subjects. It is at least logically possible that a greater proportion of fibers will be present in subjects with larger brains than others. Brains may also scale allometrically, e.g., according to a logarithmic power law. An overall larger brain does not necessarily mean that the size of each cortical region is proportionately scaled up by the same multiplicative factor. The dependency of connectivity on brain size may be a topic of future investigation.

This pilot connectivity study is limited by the relatively small number of tracts traced in these subjects, but the sample size is still very large for a 4T HARDI study (N=234). While these tracts were probabilistically seeded in regions of high anisotropy, ensuring a high probability of finding the major tracts, future studies including more tracts will allow conclusions to be made regarding connectivity in regions that were discarded in this analysis due to lack of sufficient fibers across the entire population.

REFERENCES

[1] M. Thomason and P. Thompson, "Diffusion Imaging, White Matter and Psychopathology," *Annual Review of Clinical Psychology*. in press, Oct. 2010.

[2] M. Kubicki*, et al.*, "Reduced interhemispheric connectivity in schizophrenia-tractography based segmentation of the corpus callosum," *Schizophr Res,* vol. 106, pp. 125-31, Dec 2008.

[3] T. Bitan*, et al.*, "Bidirectional connectivity between hemispheres occurs at multiple levels in language processing but depends on sex," *J Neurosci,* vol. 30, pp. 11576-85, Sep 1 2010.

[4] C. Davatzikos and S. M. Resnick, "Sex differences in anatomic measures of interhemispheric connectivity: correlations with cognition in women but not men," *Cereb Cortex,* vol. 8, pp. 635-40, Oct-Nov 1998.

[5] H. J. Park*, et al.*, "Corpus callosal connection mapping using cortical gray matter parcellation and DT-MRI," *Hum Brain Mapp,* vol. 29, pp. 503-16, May 2008.

[6] Y. P. Chao*, et al.*, "Probabilistic topography of human corpus callosum using cytoarchitectural parcellation and high angular resolution diffusion imaging tractography," *Hum Brain Mapp,* vol. 30, pp. 3172-87, Oct 2009.

[7] P. Hagmann*, et al.*, "Mapping the structural core of human cerebral cortex," *PLoS Biol,* vol. 6, p. e159, Jul 1 2008.

[8] I. Aganj*, et al.*, "A Hough transform global probabilistic approach to multiple-subject diffusion MRI tractography," Medical Image Analysis, *in press* 2011.

[9] G. I. de Zubicaray*, et al.*, "Meeting the Challenges of Neuroimaging Genetics," *Brain Imaging Behav,* vol. 2, pp. 258-263, Dec 1 2008.

[10] C. J. Holmes*, et al.*, "Enhancement of MR images using registration for signal averaging," *J Comput Assist Tomogr,* vol. 22, pp. 324-33, Mar-Apr 1998.

[11] A. Leow*, et al.*, "Inverse consistent mapping in 3D deformable image registration: its construction and statistical properties," *Inf Process Med Imaging,* vol. 19, pp. 493-503, 2005.

[12] B. Fischl*, et al.*, "Automatically parcellating the human cerebral cortex," *Cereb Cortex,* vol. 14, pp. 11-22, Jan 2004.

[13] I. Aganj*, et al.*, "Reconstruction of the orientation distribution function in single- and multiple-shell q-ball imaging within constant solid angle," *Magn Reson Med,* vol. 64, pp. 554-66, Aug 2010.

[14] D. S. Tuch, "Q-ball imaging," *Magn Reson Med,* vol. 52, pp. 1358-72, Dec 2004.

[15] P. J. Basser and C. Pierpaoli, "Microstructural and physiological features of tissues elucidated by quantitative-diffusion-tensor MRI," *J Magn Reson B,* vol. 111, pp. 209-19, Jun 1996.

[16] J. C. Pinheiro and D. M. Bates, *Mixed-effects models in S and S-PLUS*. New York: Springer, 2000.

[17] A. M. O. Veale, "Introduction to Quantitative Genetics - Falconer,Ds," *The Royal Statistical Society Series C-Applied Statistics,* vol. 9, pp. 202-203, 1960.

[18] J. B. Hellige, "Hemispheric asymmetry," *Annu Rev Psychol,* vol. 41, pp. 55-80, 1990.

[19] N. Geschwind and A. M. Galaburda, "Cerebral lateralization. Biological mechanisms, associations, and pathology: I. A hypothesis and a program for research," *Arch Neurol,* vol. 42, pp. 428-59, May 1985.

[20] D. Kimura, *Sex and cognition*. Cambridge, Mass.: MIT Press, 1999.

[21] E. Luders*, et al.*, "Gender differences in cortical complexity," *Nat Neurosci,* vol. 7, pp. 799-800, Aug 2004.

ACKNOWLEDGMENTS

This work was supported by NIH grant R01 HD050735 and the National Health and Medical Research Council, Australia, grant NHMRC 496682. Additional support was provided by grants R01 EB008281, P41 RR013642, P41 RR008079, P30 NS057091, R01 EB008432, the University of Minnesota Institute for Translational Neuroscience and NLM T15 LM07356.